


**Spin squeezing generated by the anisotropic central spin model**Lei Shao  and Libin Fu <sup>\*</sup>*Graduate School of China Academy of Engineering Physics, Beijing 100193, China* (Received 30 November 2023; accepted 1 May 2024; published 13 May 2024)

Spin squeezing, as a crucial quantum resource, plays a pivotal role in quantum metrology, enabling us to achieve high-precision parameter estimation schemes. Here, we investigate the spin squeezing and the quantum phase transition in an anisotropic central spin system. We find that this kind of central spin system can be mapped to the anisotropic Lipkin-Meshkov-Glick model in the limit where the ratio of transition frequencies between the central spin and the spin bath tends towards infinity. This property can induce a one-axis twisting interaction and provides another possibility for generating spin squeezing. We consider the generation of spin-squeezed states through the ground state and the dynamical evolution of the central spin model, respectively. The results show that the dynamical approach is more effective, and the spin-squeezing parameter improves as the anisotropy parameter decreases, while its value scales with system size as  $N^{-2/3}$ . Furthermore, we obtain the critical exponent of the quantum Fisher information around the critical point by numerical simulation, and find its value tends to  $4/3$  as the frequency ratio and the system size approach infinity. This paper offers a promising scheme for generating spin-squeezed state and paves the way for potential advancements in quantum sensing.

DOI: [10.1103/PhysRevA.109.052618](https://doi.org/10.1103/PhysRevA.109.052618)**I. INTRODUCTION**

As the understanding of the quantum world continues to deepen, quantum technology is ushering in a series of revolutionary changes in the real world. Notably, quantum precision measurement is progressively gaining prominence, especially playing a crucial role in critical areas such as biophysics [1–4], inertial sensors [5,6], and measurement of physics constants [7–9]. In the realm of quantum metrology, a core goal is to improve the measurement precision of the parameters of interest. As a result, a central focus of research lies in exploring how to utilize the nonclassical properties of quantum resources to achieve heightened precision. In the past decades, quantum spin squeezing has garnered considerable attention as an important concept in the field of quantum information, particularly in quantum metrology and quantum sensing. Due to its capability to reduce quantum fluctuations of a specific spin component, spin squeezing can enhance the precision of measurements, thus spin-squeezed states are widely applied in the domain of quantum precision measurement, such as atomic clock [10–12], Ramsey spectroscopy [13–17], and gravitational wave interferometers [18–20]. Furthermore, investigating spin squeezing is also helpful to gain a deeper understanding of the correlations, entanglement, and quantum information processing among particles in quantum systems [21–24].

The generation of spin squeezing involves two categories [25], including nonlinear atomic-atomic collisions in Bose-Einstein condensates (BECs) [26–36] and atomic-photon interactions [37–53]. The former exploits the nonlinear effects of atomic collisions to generate spin-squeezed states, while the latter mainly involves utilizing squeezing transfer from the

optical field to spin ensemble [38,46,48,51,52], the coherent feedback of the optical cavity [47,53], or quantum nondemolition (QND) measurement of the output light [43,49,50,52].

Utilizing bosonic atoms to generate spin squeezing can result in more losses due to collisions [54–56], hence it is essential to explore the use of spinful fermions to achieve spin squeezing. Due to the similarity between the light-matter interaction and the spin-spin interaction, the central spin systems can also induce a one-axis twisting (OAT) interaction under certain conditions, thus it can be regarded as a promising alternative model to realize spin squeezing. The scheme proposed in Ref. [57] innovatively employed a similar approach to achieve spin squeezing in a quantum dot composed of an electron and a large ensemble of nuclear spins. However, the mechanism of inducing the effective one-axis twisting interaction in central spin systems is still ambiguous, thus, we employ the Schrieffer-Wolff transformation to rigorously illustrate the generation mechanism of the OAT interaction and extend it to the anisotropic case. We find that when the ratio of the transition frequency of the central spin to that of the bath spin tends to infinity, the anisotropic central spin model can be mapped to the anisotropic Lipkin-Meshkov-Glick (LMG) model [58], where the OAT interaction in the Hamiltonian can dynamically generate spin squeezing. In addition, there exists a quantum phase transition (QPT) in this anisotropic central spin model, and its quantum criticality can be viewed as a quantum resource for quantum metrology. Thus we investigate the finite-size behavior around the critical point and numerically calculate the critical exponent of the quantum Fisher information (QFI). It is found that when the frequency ratio tends to infinity, the critical adiabatic dimension of the central spin model become equal to those of the LMG model, however, as the frequency ratio decreases, the corresponding exponent will decay to zero.

<sup>\*</sup>lbfu@gascaep.ac.cn

This paper is organized as follows. In Sec. II, we give the derivation of the mapping between the anisotropic central spin model and the anisotropic LMG model. In Sec. III, we investigate the spin squeezing and quantum phase transitions of the central spin model under both isotropic and anisotropic conditions. In Sec. IV, we discuss the quantum Fisher information and its critical exponent of the ground state in the anisotropic central spin model. Finally, we give a conclusion in Sec. V.

## II. MODEL

The central spin model can be described as an ensemble of  $N$  identical spin- $\frac{1}{2}$  particles with a total spin of  $I = N/2$  interacting with a central spin- $\frac{1}{2}$  particle. This model is discussed in Refs. [59–65] and its Hamiltonian can be written as (we set  $\hbar = 1$ )

$$H = \frac{\Omega}{2}\sigma_z^{(0)} + \frac{\omega}{2}\sum_{k=1}^N\sigma_z^{(k)} + \sum_{k=1}^N\left(\frac{A_x}{2}\sigma_x^{(k)}\sigma_x^{(0)} + \frac{A_y}{2}\sigma_y^{(k)}\sigma_y^{(0)} + \frac{A_z}{2}\sigma_z^{(k)}\sigma_z^{(0)}\right), \quad (1)$$

where  $\Omega$  and  $\omega$  are the transition frequencies of the central spin and bath spins induced by an external magnetic field, respectively.  $A_i$  ( $i = x, y, z$ ) represents the strength of the interaction between the central spin and bath spins in different directions. Here,  $\sigma_i^{(0)}$  represents the Pauli operator of the central spin and  $\sigma_i^{(k)}$  ( $k \neq 0, i = x, y, z$ ) is the  $i$ th Pauli operator of the bath spins. The central spin model is widely used to study the spin-spin interactions in quantum dots [62,62–64] and nitrogen-vacancy centers [65]. Some intriguing physical phenomena, such as collapse and revival [59,60], the super-radiance effect [59], and dissipative phase transitions [66], emerge within this model. In this paper, we mainly focus on the anisotropic model, that is, the coupling strength of the  $X$  and  $Y$  directions is different. Hence we set  $A_x = (1 + \lambda)A$ ,  $A_y = (1 - \lambda)A$ , and  $A_z = 0$ , and Eq. (1) can be rewritten as

$$H = \frac{\Omega}{2}\sigma_z + \omega I_z + A[(I_+\sigma_- + I_-\sigma_+) + \lambda(I_+\sigma_+ + I_-\sigma_-)], \quad (2)$$

where  $\sigma_z^{(0)} \equiv \sigma_z$ ,  $I_i = \frac{1}{2}\sum_{k=1}^N\sigma_i^{(k)}$ , and  $\lambda$  is the anisotropy parameter. Note that the Hamiltonian in Eq. (2) commutes with the operators  $\mathcal{P}_1 = \exp[i\pi(\sigma_z/2 + I_z + N/2)]$  and  $\mathcal{P}_2 = \prod_{i=0}^N\sigma_z^{(i)}$ , i.e.,  $[H, \mathcal{P}_1] = [H, \mathcal{P}_2] = 0$ , indicating that it possesses the  $Z_2$  symmetry (spin-flip symmetry). This  $Z_2$  symmetry also leads to the following consequence for any eigenstates of  $\mathcal{P}_2$  that satisfy [67,68]

$$\left\langle \sum_{i=0}^N \sigma_x^{(i)} \right\rangle = \left\langle \sum_{i=0}^N \sigma_y^{(i)} \right\rangle = 0. \quad (3)$$

It can be seen that if the anisotropy parameter  $\lambda = 1$ , then the total magnetization  $M = \sigma_z/2 + I_z$  remains invariant under the action of this Hamiltonian. This allows us to find a two-dimensional subspace to solve the eigenstates of the Hamiltonian in Eq. (2). However, if  $\lambda \neq 1$ , then such a closed subspace does not exist, which complicates further analysis of

this model. To this end, we apply a Schrieffer-Wolff transformation  $e^S$  with  $S = -iA(1 + \lambda)/\Omega I_x \sigma_y + iA(1 - \lambda)/\Omega I_y \sigma_x$  to Eq. (2), and in the limit of  $\eta = \Omega/\omega \rightarrow \infty$  we obtain

$$H = \frac{\Omega}{2}\sigma_z + \gamma_z I_z + \frac{1}{N}(\gamma_x I_x^2 + \gamma_y I_y^2)\sigma_z, \quad (4)$$

where

$$\gamma_x = \frac{\tilde{g}^2\omega(1 + \lambda)^2}{4}, \quad \gamma_y = \frac{\tilde{g}^2\omega(1 - \lambda)^2}{4}, \quad (5)$$

$$\gamma_z = \omega - \tilde{g}^2\frac{(1 + \lambda)(1 - \lambda)\omega}{4N}, \quad (6)$$

$$\tilde{g} = \frac{2A\sqrt{N}}{\sqrt{\Omega\omega}}. \quad (7)$$

Here,  $\tilde{g}$  in Eq. (7) is a dimensionless coupling strength parameter. It can be seen that the Hamiltonian in Eq. (4) is block-diagonal with respect to spin states and its low-energy effective Hamiltonian in the spin-down subspace is

$$H_{\downarrow} = -\frac{\Omega}{2} + \gamma_z I_z - \frac{1}{N}(\gamma_x I_x^2 + \gamma_y I_y^2). \quad (8)$$

One can see that Eq. (8) is exactly the Hamiltonian of the anisotropic LMG model. In other words, there exists a mapping between the anisotropic model and the LMG model in the limit of  $\eta \rightarrow \infty$ . The detailed derivation of the above process is presented in Appendix A. A similar method for generating spin squeezing has been discussed in Ref. [57]. Here, we present an explicit mapping relationship coupled with the corresponding derivation process.

## III. SPIN SQUEEZING AND QUANTUM PHASE TRANSITIONS IN CENTRAL SPIN MODEL

In this section, we will discuss the spin squeezing and quantum phase transition in the anisotropic central spin model. We will begin by introducing the two commonly used definitions of spin squeezing proposed by Kitagawa *et al.* [69] and Wineland *et al.* [70], which are given by

$$\xi_S^2 = \frac{4 \min(\Delta^2 I_{\bar{n}_{\perp}})}{N}, \quad (9)$$

and

$$\xi_R^2 = \frac{N \min(\Delta^2 I_{\bar{n}_{\perp}})}{|\langle \vec{I} \rangle|^2}, \quad (10)$$

where  $\bar{n}_{\perp}$  refers to an axis perpendicular to the mean spin direction  $\langle \vec{I} \rangle$  with  $\vec{I} = (I_x, I_y, I_z)$ ,  $\Delta^2 I_{\bar{n}_{\perp}}$  is the variance of  $I_{\bar{n}_{\perp}} = \vec{I} \cdot \bar{n}_{\perp}$ , and the minimization is over all directions  $\bar{n}_{\perp}$ . If  $\xi_S^2 < 1$  or  $\xi_R^2 < 1$ , it implies that this state is a spin-squeezed state. Moreover, there exist other definitions of spin-squeezing parameters, as discussed in Refs. [23,26,71–74], which have been employed to investigate the relationship between entanglement and spin squeezing. In the following, we will analyze the spin squeezing in the isotropic ( $\lambda = 0$ ) and anisotropic ( $\lambda \neq 0$ ) cases separately.

### A. Isotropic case

For  $\lambda = 0$ , the Hamiltonian in Eq. (2) becomes

$$H = \frac{\Omega}{2}\sigma_z + \omega I_z + \frac{\tilde{g}}{2}\sqrt{\frac{\Omega\omega}{N}}(I_+\sigma_- + I_-\sigma_+). \quad (11)$$

We can find that the above Hamiltonian remains invariant under the action of  $\Pi = \exp[i\theta(\sigma_z/2 + I_z + N/2)]$ , indicating that it possesses  $U(1)$  symmetry. In Sec. II, we mention that the Hamiltonian in Eq. (11) can be solved by utilizing a closed subspace. The analytical solution of isotropic case has been discussed in detail in Refs. [60,61].

First, we will briefly review the results presented in Ref. [61] and calculate the spin-squeezing parameters of the ground state in the isotropic case. Reference [61] shows that there exists a normal-to-superradiant phase transition in the limit of  $\eta \rightarrow \infty$  and  $N \rightarrow \infty$ , and the critical point is  $\tilde{g}_c = 2/(1 + \lambda) = 2$ . For further analysis, we introduce the Dicke state  $|n\rangle \equiv |\frac{N}{2}, -\frac{N}{2} + n\rangle$  ( $n \in [0, N]$ ), which is the eigenstate of the operators  $I^2$  and  $I_z$ . For  $\eta \gg 1$  and  $N \gg 1$ , the ground state is  $|\downarrow, 0\rangle \equiv |\downarrow\rangle \otimes |\frac{N}{2}, -\frac{N}{2}\rangle$  when  $\tilde{g} < 2$ , where  $|\downarrow\rangle$  ( $|\uparrow\rangle$ ) is the eigenstate of the operator  $\sigma_z$ . Immediately, we obtain  $\xi_S^2 = \xi_R^2 = 1$  under the condition of  $\tilde{g} < 2$ . For  $\tilde{g} > 2$ , the ground state is given by [61]

$$|\psi_{-}(n)\rangle = \tilde{P}_{\uparrow, n-1}|\uparrow, n-1\rangle + \tilde{P}_{\downarrow, n}|\downarrow, n\rangle, \quad (12)$$

where

$$\tilde{P}_{\uparrow, n-1} = \frac{\tilde{\Omega} - \sqrt{1 + \tilde{\Omega}^2}}{\sqrt{2(1 + \tilde{\Omega}^2) - 2\tilde{\Omega}\sqrt{1 + \tilde{\Omega}^2}}}, \quad (13)$$

$$\tilde{P}_{\downarrow, n} = \frac{1}{\sqrt{2(1 + \tilde{\Omega}^2) - 2\tilde{\Omega}\sqrt{1 + \tilde{\Omega}^2}}}, \quad (14)$$

$$\tilde{\Omega} = \frac{\Omega - \omega}{\tilde{g}\sqrt{(N - n + 1)n\Omega\omega}}, \quad (15)$$

and

$$n = \frac{\eta}{4}(\tilde{g}^2 - \tilde{g}^{-2}). \quad (16)$$

Here,  $n$  in Eq. (16) can be regarded as the excitation number of the ground state. Utilizing the above equations, we can obtain the spin-squeezing parameters of the ground state for  $\eta \gg 1$ , which are

$$\xi_S^2 = -\frac{2(n - \frac{N}{2})^2}{N} + \frac{N}{2} + 1, \quad (17)$$

and

$$\xi_R^2 = -\frac{N}{2} + \frac{N^2(N + 2)}{8(n - \frac{N}{2})^2}. \quad (18)$$

The derivation of the above equations is provided in Appendix B. The analytical results of Eqs. (17) and (18) are shown in Fig. 1. One can see that the squeezing parameters  $\xi_S^2$  and  $\xi_R^2$  remain 1 when  $\tilde{g} < \tilde{g}_c$ , and they begin to continuously increase after crossing the critical point  $\tilde{g}_c$ , which implies that the squeezing parameters can be used as an indicator to characterize the phase transition [25,68,75]. Apart from this, we can also find that the squeezing parameters of the central spin model tend to approach those of the LMG model as the

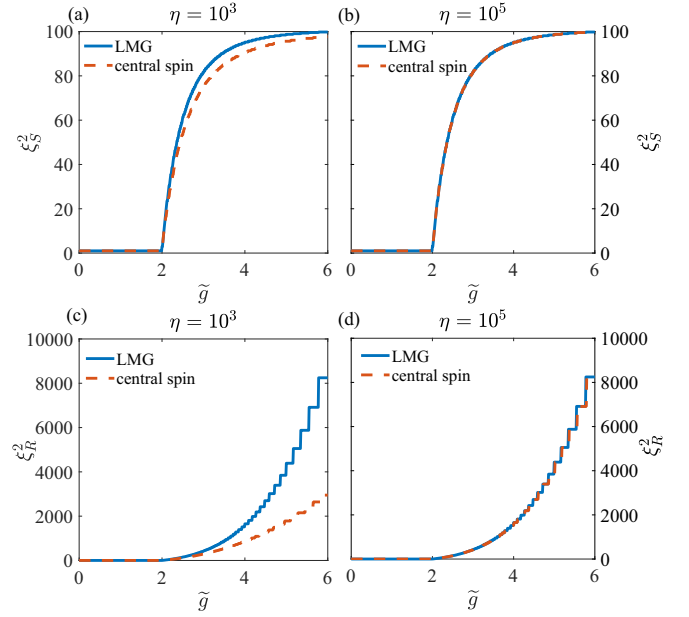


FIG. 1. Spin-squeezing parameters  $\xi_S^2$  and  $\xi_R^2$  of the ground state for the isotropic case as functions of  $\tilde{g}$  with  $N = 200$ . The first row [(a) and (b)] corresponds to the cases of spin-squeezing parameter  $\xi_S^2$  with  $\eta = 10^3$  and  $\eta = 10^5$ , respectively. The second row [(c) and (d)] corresponds to the cases of spin-squeezing parameter  $\xi_R^2$  with  $\eta = 10^3$  and  $\eta = 10^5$ , respectively. The solid lines are the results of the LMG model and the dashed lines are the results of the central spin model.

frequency ratio  $\eta$  increases. As shown in Figs. 1(b) and 1(d), the two spin-squeezing parameters are essentially consistent when the frequency ratio is  $\eta = 10^5$ .

However, from the above analysis, we can find that the ground state of the central spin model is not a spin-squeezed state due to  $\xi_R^2 \geq \xi_S^2 \geq 1$ . Subsequently, we will explore the possibility of generating spin-squeezed states through a dynamical approach. We choose  $|\downarrow\rangle \otimes |\psi_{cs}\rangle$  as the initial state, where  $|\psi_{cs}\rangle$  is the spin coherent state, i.e.,  $|\psi_{cs}\rangle = \otimes_{k=0}^N [\cos(\theta_0/2)|\uparrow\rangle_k + e^{i\phi_0}(\theta_0/2)|\downarrow\rangle_k]$ , and the exact solution of this dynamical process has been provided in Ref. [60], which is

$$|\psi_f(t)\rangle = \sum_{m=0}^N \sqrt{C_N^m} e^{-i(-\frac{N}{2} + m - \frac{1}{2})\omega t} \left(\cos \frac{\theta_0}{2}\right)^m \left(\sin \frac{\theta_0}{2}\right)^{N-m} \times (P_{\downarrow}^m |\downarrow, m\rangle + P_{\uparrow}^m |\uparrow, m-1\rangle), \quad (19)$$

where  $P_{\downarrow}^m = i\Omega \sin(\Omega_m t/2)/\Omega_m + \cos(\Omega_m t/2)$ ,  $P_{\uparrow}^m = -i2\sqrt{k_m}A \sin(\Omega_m t/2)/\Omega_m$ , and  $\Omega_m = \sqrt{\Omega^2 + 4k_m A^2}$  with  $k_m = m(N - m + 1)$ . Note that we set  $\phi_0 = 0$  for simplicity, and the mean spin direction is  $\bar{n}_0 = (\sin \theta \cos \phi, \sin \theta \sin \phi, \cos \theta)$ , while the directions perpendicular to it are given by  $\bar{n}_1 = (-\sin \phi, \cos \phi, 0)$  and  $\bar{n}_2 = (\cos \theta \cos \phi, \cos \theta \sin \phi, -\sin \theta)$ , where the parameters  $\theta(t)$  and  $\phi(t)$  are functions of evolution time  $t$ . The spin-squeezing parameters are given by [76]

$$\xi_S^2 = \frac{2(C - \sqrt{A^2 + B^2})}{N}, \quad (20)$$

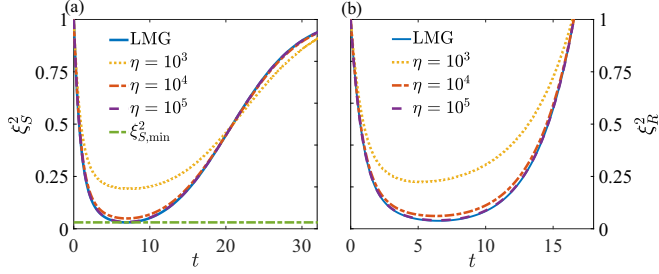


FIG. 2. Time evolution of the spin-squeezing parameters  $\xi_S^2$  [(a)] and  $\xi_R^2$  [(b)] for different frequency ratios  $\eta$ . The parameters chosen here are  $N = 200$ ,  $\omega = 1$ , and  $\tilde{g} = 2$ . The curves from top to bottom correspond to the spin-squeezing parameter  $\xi_S^2$  of the LMG model (blue solid line) and the central spin model with frequency ratios  $\eta = 10^3$  (yellow dotted line),  $\eta = 10^4$  (red dashed-dotted line), and  $\eta = 10^5$  (purple dashed line), respectively. In (a), the bottom straight line corresponds to the optimal spin-squeezing parameter  $\xi_{S,\min}^2$  (green dashed-dotted line).

and

$$\xi_R^2 = \frac{N^2}{4|\langle \tilde{I} \rangle|^2} \xi_S^2, \quad (21)$$

where  $\mathcal{A} = \langle I_{\bar{n}_1}^2 - I_{\bar{n}_2}^2 \rangle$ ,  $\mathcal{B} = \langle I_{\bar{n}_1} I_{\bar{n}_2} - I_{\bar{n}_2} I_{\bar{n}_1} \rangle$ ,  $\mathcal{C} = \langle I_{\bar{n}_1}^2 + I_{\bar{n}_2}^2 \rangle$ . The values of the above parameters only depend on the following five parameters:  $\langle I_z \rangle$ ,  $\langle I_z^2 \rangle$ ,  $\langle I_+ \rangle$ ,  $\langle I_+^2 \rangle$ ,  $\langle I_+(2I_z + 1) \rangle$  [76]. The specific expressions for the above parameters are presented in Appendix B. Due to the inequality  $\xi_S^2 \leq \xi_R^2$ , as long as the quantum state satisfies  $\xi_S^2 < 1$ , then this state can be regarded as a spin-squeezed state. Therefore, we only need to compute  $\xi_S^2$  from now on.

In Fig. 2, we show time evolution of the spin-squeezing parameters  $\xi_S^2$  and  $\xi_R^2$  of the central spin model with different frequency ratios  $\eta$ . Here, we choose  $\theta_0 = \pi/2$  and  $N$  is large enough ( $N = 200$ ), and the optimal squeezing parameter for the above model is given by

$$\xi_{S,\min}^2 \simeq \frac{1}{2} \left( \frac{N}{3} \right)^{-\frac{2}{3}}, \quad (22)$$

and the corresponding squeezing time is

$$t_{\min} \simeq \frac{4 \times 3^{\frac{1}{6}} N^{\frac{1}{3}}}{\tilde{g}^2 \omega}. \quad (23)$$

In fact, for the OAT interaction, i.e.,  $\chi I_z^2$ , it has the following power-law scalings with respect to  $N$ :  $\xi_{S,\min}^2 \sim N^{-2/3}$  and  $\chi t_{\min} \sim N^{-2/3}$  [69,76–78]. From Eqs. (22) and (23), we can see that the power-law scalings of  $\xi_{S,\min}^2$  and  $t_{\min}$  (here,  $\chi = \tilde{g}^2 \omega / 4N$ ) are the same as the one-axis twisting case when  $\eta$  is sufficiently large. On the other hand, a substantial detuning between the central spin and bath spins ( $\Omega/\omega \gg 1$ ) can induce an intraspecies interaction, which is reported in Refs. [57,79].

### B. Anisotropic case

Now we consider the anisotropic case, and without loss of generality we set  $0 < \lambda \leq 1$ . For the Hamiltonian in Eq. (2), it is difficult to obtain its analytical solution. To further analyze it, we begin with the Hamiltonian in Eq. (8) ( $\eta \rightarrow \infty$ ) and

employ the mean-field approximation [67,68] to obtain the following mean-field energy,

$$\begin{aligned} E_{\text{MF}} &= \langle \psi_{\text{cs}} | H | \psi_{\text{cs}} \rangle \\ &= \frac{N\omega}{2} \cos \theta_0 - \frac{\tilde{g}^2 N \omega \sin^2 \theta_0}{16} (1 + \lambda^2 + 2\lambda \cos 2\phi_0) \\ &\geq \frac{\gamma_x N}{4} \left( \cos \theta_0 + \frac{\omega}{\gamma_x} \right)^2 - \frac{N\omega^2}{4\gamma_x} - \frac{\gamma_x N}{4}, \end{aligned} \quad (24)$$

where  $|\psi_{\text{cs}}\rangle$  is the spin coherent state. In the limit of  $\eta \rightarrow \infty$  and  $N \rightarrow \infty$ , the collective spin operators  $I_i$  ( $i = x, y, z$ ) in Eq. (8) can be treated as classical variables, thus we can minimize the mean-field energy  $E_{\text{MF}}$  by varying  $\theta_0$  and  $\phi_0$ , thereby distinguishing between the two different phases.

In order to minimize the energy, we find the following conditions: (i) For  $\tilde{g} < 2/(1 + \lambda)$ , we have  $\theta_0 = \pi$  and  $\phi_0$  is arbitrary; (ii) for  $\tilde{g} > 2/(1 + \lambda)$ , we have  $\theta_0 = \arccos(-\omega/\gamma_x)$ , and  $\phi_0 = 0, \pi$ . Furthermore, we rotate the spin operators around the  $y$  axis to align the  $z$  axis with the direction of the semiclassical magnetization. The rotated operators are expressed as  $\tilde{I}_x = \cos \theta_0 I_x - \sin \theta_0 I_z$ ,  $\tilde{I}_y = I_y$ , and  $\tilde{I}_z = \sin \theta_0 I_x + \cos \theta_0 I_z$ , and the Hamiltonian in Eq. (8) becomes

$$\begin{aligned} H_{\downarrow} &= -\frac{\gamma_x}{N} [\cos^2 \theta_0 \tilde{I}_x^2 + \sin^2 \theta_0 \tilde{I}_z^2 + \sin \theta_0 \cos \theta_0 (\tilde{I}_x \tilde{I}_z + \tilde{I}_z \tilde{I}_x)] \\ &\quad - \frac{\gamma_y}{N} \tilde{I}_y^2 + \gamma_z (-\sin \theta_0 \tilde{I}_x + \cos \theta_0 \tilde{I}_z). \end{aligned} \quad (25)$$

Then we apply the Holstein-Primakoff transformation to the above equation, i.e.,  $\tilde{I}_+ = \sqrt{Na}a$ ,  $\tilde{I}_- = \sqrt{Na}a^\dagger$ , and  $\tilde{I}_z = N/2 - a^\dagger a$ , and assume that  $N$  is sufficiently large ( $\sqrt{a^\dagger a}/N \simeq 1$ ,  $\gamma_z \simeq \omega$ ), then Eq. (25) can be rewritten as

$$H_{\downarrow} = -\frac{\gamma_x}{2} \cos^2 \theta_0 x^2 - \frac{\gamma_y}{2} p^2 + (\gamma_x \sin^2 \theta_0 - \omega \cos \theta_0) a^\dagger a, \quad (26)$$

where  $x = (a^\dagger + a)/\sqrt{2}$  and  $p = i(a^\dagger - a)/\sqrt{2}$ . In the above derivation, we utilize  $\omega \sin \theta_0 + \gamma_x \sin \theta_0 \cos \theta_0 = 0$  and keep the terms up to order  $(1/N)^{-1/2}$ , while neglecting the constant terms and the higher-order terms  $O[(1/N)^{1/2}]$ .

Similar to the isotropic case, the spin-squeezing parameter differs before and after the critical point. First, for  $\tilde{g} < 2/(1 + \lambda)$  and  $\theta_0 = \pi$ , Eq. (26) becomes

$$\bar{H} = \omega a^\dagger a - \frac{1}{2} (\gamma_x x^2 + \gamma_y p^2). \quad (27)$$

Then we use a unitary transformation with a squeezing operator  $\mathcal{S}(r) = \exp[(r/2)(a^2 - a^{\dagger 2})]$  to Eq. (27) and obtain

$$\bar{H}' = \sqrt{(\omega - \gamma_x)(\omega - \gamma_y)} (a^\dagger a + \frac{1}{2}), \quad (28)$$

where  $r = \frac{1}{4} \ln[(\omega - \gamma_x)/(\omega - \gamma_y)]$ . It is worth noting that the ground state of the Hamiltonian in Eq. (8) satisfies that  $\langle \{I_x, I_y\} \rangle = 0$ , thus the spin-squeezing parameter is given by [68]

$$\xi_S^2 = \frac{4 \min \{ \langle I_x^2 \rangle, \langle I_y^2 \rangle \}}{N}, \quad (29)$$

where  $\langle I_x^2 \rangle = \langle \tilde{I}_x^2 \rangle = Ne^{-2r}/4$  and  $\langle I_y^2 \rangle = \langle \tilde{I}_y^2 \rangle = Ne^{2r}/4$ . Utilizing the above equations, we ultimately obtain the



spin-squeezing parameter is given by

$$\xi_S^2 = \left( \frac{\tilde{g}_c^2 - \tilde{g}^2}{\tilde{g}_c^2 - \gamma \tilde{g}^2} \right)^{\frac{1}{2}}, \quad (30)$$

where  $\gamma = \gamma_y/\gamma_x$ . For  $\tilde{g} > 2/(1 + \lambda)$  and  $\theta_0 = \arccos(-\omega/\gamma_x)$ , Eq. (26) becomes

$$\tilde{H} = \frac{\omega}{2} \left( \frac{\gamma_x}{\omega} - \frac{\omega}{\gamma_x} \right) x^2 + \frac{\tilde{g}^2 \omega \lambda}{2} p^2 - \frac{\gamma_x}{2}. \quad (31)$$

Similarly, by applying a squeezing operator  $\mathcal{S}(r)$  to Eq. (31), we obtain

$$\tilde{H}' = \omega \sqrt{\tilde{g}^2 \lambda \left( \frac{\gamma_x}{\omega} - \frac{\omega}{\gamma_x} \right)} \left( a^\dagger a + \frac{1}{2} \right) - \frac{\gamma_x}{2}, \quad (32)$$

where  $r = \frac{1}{4} \ln[(\gamma_x/\omega - \omega/\gamma_x)/\tilde{g}^2 \lambda]$ . The corresponding spin-squeezing parameter is

$$\xi_S^2 = \left[ \frac{1}{\tilde{g}^2 \lambda} \left( \frac{\tilde{g}^2}{\tilde{g}_c^2} - \frac{\tilde{g}_c^2}{\tilde{g}^2} \right) \right]^{\frac{1}{2}}. \quad (33)$$

For the spin-squeezing parameter  $\xi_S^2$ , it can be obtained through Eq. (21), where

$$|\langle \vec{I} \rangle| = \begin{cases} \frac{N}{2} - \sinh^2 r, & \tilde{g} \leq \tilde{g}_c, \\ \frac{\omega}{\gamma_x} \left( \frac{N}{2} - \sinh^2 r \right), & \tilde{g} > \tilde{g}_c. \end{cases} \quad (34)$$

From Eqs. (30) and (33), we can see that  $\xi_S^2 < 1$  when  $\tilde{g} < 2/\sqrt{(1 + \lambda)(1 - \lambda)}$ , which implies that one can generate the spin-squeezed state by preparing the ground state of the anisotropic central spin model with a large frequency ratio  $\eta$ . In Fig. 3(a), we present the spin-squeezing parameter  $\xi_S^2$  of the ground state for the anisotropic case varies with  $\tilde{g}$ . It can be seen that the spin-squeezing parameter  $\xi_S^2$  of the anisotropic central spin model tends to that of the LMG model as the frequency ratio  $\eta$  increases.

In Fig. 3(a), it is evident that the optimal squeezing parameter appears in the vicinity of the critical point. However, one can see that the analytical expression of  $\xi_S^2$  (solid green line) decreases to zero at the critical point, which means the results of Eqs. (30) and (33) fail when  $\tilde{g}$  approach  $\tilde{g}_c$ . It implies that merely considering the retained terms in Eq. (26) is insufficient. In such a case, it is necessary to consider the higher-order corrections. The calculation method for the higher-order terms requires the utilization of the continuous unitary transformation, which is discussed in Ref. [67]. Here, we directly employ a numerical simulation to calculate the variation of the optimal spin-squeezing parameter  $\xi_{S,\min}^2$  at the critical point with respect to  $N$ , and the corresponding log-log plot is shown in Fig. 3(b). The slopes of the fitted lines with different  $\eta$  are separately  $-0.2334$  ( $\eta = 10^3$ ),  $-0.3096$  ( $\eta = 10^4$ ), and  $-0.3208$  ( $\eta = 10^5$ ) for  $N$  scaling. In the limit of  $\eta \rightarrow \infty$ , we have  $\xi_{S,\min}^2 \sim N^{-1/3}$ , which is consistent with the result of the LMG model in Refs. [25,80].

The spin-squeezing parameters of the dynamic process with various  $\lambda$  are also investigated by numerical simulation. In Fig. 3(c), we compare the dynamical evolution of spin-squeezing parameter  $\xi_S^2$  with different values of  $\lambda$ . It is clear that as the value of  $\lambda$  decreases, the corresponding optimal

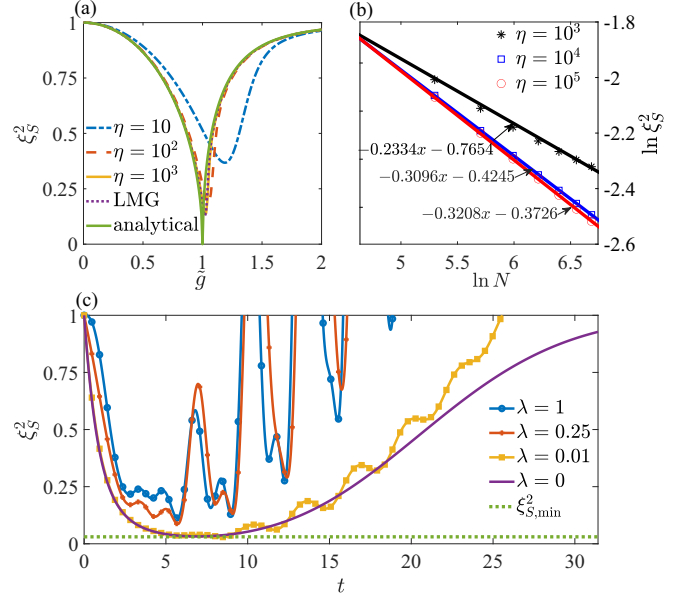


FIG. 3. (a) Spin-squeezing parameter  $\xi_S^2$  of the ground state for the anisotropic case as functions of  $\tilde{g}$  with different frequency ratios  $\eta$ . Here, we choose  $N = 200$ ,  $\omega = 1$ , and  $\lambda = 1$ . The curves from top to bottom correspond to the spin-squeezing parameter  $\xi_S^2$  of the central spin model with frequency ratios  $\eta = 10$  (blue dashed-dotted line),  $\eta = 10^2$  (red dashed line), and  $\eta = 10^3$  (yellow solid line), the LMG model (purple dotted line), and the analytical results given by Eqs. (30) and (33) (solid green line), respectively. (b) Optimal squeezing parameters  $\xi_{S,\min}^2$  of the ground state as functions of  $\ln N$  with different frequency ratios  $\eta$ . (c) Time evolution of the spin-squeezing parameters for different anisotropy parameters. The curves from top to bottom correspond to  $\lambda = 1$  (blue circle line),  $\lambda = 0.25$  (blue circle line),  $\lambda = 0.01$  (yellow point line),  $\lambda = 0$  (purple solid line).

squeezing parameter also decreases. In other words, for  $\lambda = 0$ , the associated optimal squeezing parameter  $\xi_{S,\min}^2$  is minimal.

In summary, our analysis of the above results reveals that, under the condition of fixed  $N$ , the most effective method for generating the optimal spin-squeezed state is through the dynamic evolution of the isotropic central spin model. In this process, it is crucial to make the ratio  $\eta$  between the frequency of the central spin and that of the bath spin as large as possible. The corresponding results are shown in Table I.

#### IV. QUANTUM FISHER INFORMATION AND FINITE-SIZE ANALYSIS

Quantum Fisher information is a core concept in quantum metrology, and the QFI of the ground state can be regarded

TABLE I. Spin squeezing  $\xi_S^2$  generated by the ground state and dynamical evolution in the isotropic ( $\lambda = 0$ ) and anisotropic ( $\lambda \neq 0$ ) cases.

$\xi_S^2$	Isotropic	Anisotropic
Ground state	$> 1$	$\sim N^{-\frac{1}{3}}$
Dynamical evolution	$\frac{1}{2} \left( \frac{N}{3} \right)^{-\frac{2}{3}}$	$> \frac{1}{2} \left( \frac{N}{3} \right)^{-\frac{2}{3}}$

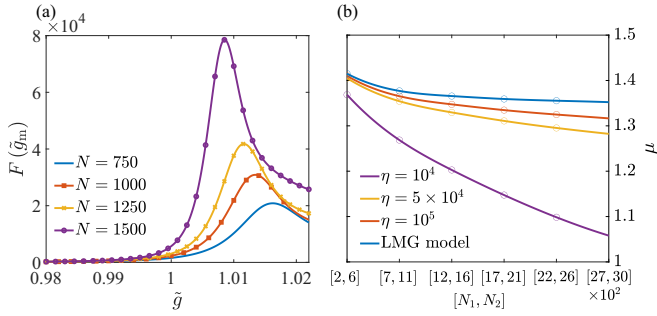


FIG. 4. (a) QFI of the ground state as functions of  $\tilde{g}$  with different numbers of bath spins  $N$ . Here, we choose  $\eta = 10^5$ ,  $\omega = 1$ ,  $\lambda = 1$ , and  $\tilde{g}_c = 1$ . The curves from top to bottom correspond to the QFI of the central spin model with  $N = 750$  (purple line),  $N = 1000$  (yellow line), and  $N = 1250$  (red line) and  $N = 1500$  (blue line), respectively. (b) Critical exponent  $\mu$  within various system sizes  $[N_1, N_2]$ . The curves from top to bottom correspond to the cases of  $\eta = 1000$  (blue line),  $\eta = 10\,000$  (red line), and  $\eta = 50\,000$  (yellow line), respectively. In addition, the case of the LMG model is also presented for comparison (top blue line).

as an indicator to detect the quantum phase transition even without knowing the information related to the order parameter [81]. Therefore, in this section, we will utilize QFI to analyze the finite-size behavior of the anisotropic central spin model. The finite-size analysis of the isotropic case ( $\lambda = 0$ ) has been discussed in Ref. [61], thus here we will focus on the anisotropic case ( $\lambda \neq 0$ ).

For a pure state  $|\psi(\tilde{g})\rangle$ , the QFI with respect to parameter  $\tilde{g}$  is give by

$$F(\tilde{g}) = 4\langle\partial_{\tilde{g}}\psi|\partial_{\tilde{g}}\psi\rangle - 4|\langle\partial_{\tilde{g}}\psi|\psi\rangle|^2, \quad (35)$$

and its value is four times the fidelity susceptibility [81,82]. According to the conclusion in Ref. [83], for the LMG model, the QFI of the ground state around the critical point presents scaling behavior as

$$F(\tilde{g}_m) \propto N^\mu, \quad (36)$$

where  $\tilde{g}_m$  is the position of the maximal QFI,  $N$  is the size of the system, and  $\mu$  is the critical adiabatic dimension with a specific value of  $\mu = 4/3$  [81]. For the anisotropic central spin model, two conditions are required for a phase transition to occur, namely, the frequency ratio  $\eta$  and the size of the system  $N$  tend to infinity. Nevertheless, when the frequency ratio  $\eta$  is finite, the scaling behavior of  $F(\tilde{g}_m)$  in Eq. (36) is still unknown. Therefore, we utilize the exact diagonalization to obtain the ground state and calculate the critical adiabatic dimension  $\mu$  for a finite  $\eta$ .

In Fig. 4(a), we depict the variation of the QFI of the ground state for the anisotropic central spin model with different numbers of bath spins. It is observed that as  $N$  increases, the maximum values of the QFI exhibits a progressively growing trend, and their corresponding positions gradually approach the critical point. The critical adiabatic dimension  $\mu$  within different system size ranges  $[N_1, N_2]$  is provided in Fig. 4(b). It is evident that, as the frequency ratio  $\eta$  increases, the value of  $\mu$  converges to  $4/3$  when  $N$  is sufficiently large, which corresponds precisely to the critical adiabatic

dimension of the LMG model (solid blue line) [83]. On the other hand, we find that if  $\eta$  is not sufficiently large, the value of  $\mu$  will rapidly decrease with increasing  $N$  until it converges to zero. Namely, if  $N$  tends to infinity while  $\eta$  remains finite, the corresponding  $\mu$  will decay to zero, which implies that the quantum phase transition will not occur. Hence, the condition for the phase transition to occur requires  $\eta$  and  $N$  both tend towards infinity.

## V. CONCLUSION

In summary, we have analyzed the spin squeezing and quantum phase transition in the anisotropic central spin model. Utilizing the Schrieffer-Wolff transformation, we analytically established the mapping between the anisotropic central spin model and the anisotropic LMG model. Meanwhile, it is shown that the substantial detuning between the central spin and bath spins can induce an intraspecies nonlinear interaction. Inspired by the above results, we investigated the potential pathways for generating spin-squeezed states with central spin systems. Through comparisons, we found that the dynamics initiated with a spin coherent state can generate the optimal spin-squeezed state. Furthermore, when the anisotropy parameter  $\lambda$  is zero, the optimal spin-squeezing parameter scales with the system size as  $N^{-2/3}$ . The critical adiabatic dimension  $\mu$  of the quantum Fisher information around the critical point has also been employed to study the finite-size behavior in the anisotropic central spin model. Specifically, we obtained  $\mu = 4/3$  as  $\eta$  and  $N$  approach infinity, however, when  $\eta$  is finite, it is found that the value of  $\mu$  decreases to zero with the increase of  $N$ . This work provides another potential pathway for generating spin-squeezed states in practical physical systems, simultaneously offering a fresh perspective for our understanding of the relationship between spin squeezing and quantum criticality.

## ACKNOWLEDGMENTS

We acknowledge Dr. Zhucheng Zhang for valuable suggestions. This work was supported by the National Natural Science Foundation of China (Grants No. 12088101, No. U2330401, and No. 12347127).

## APPENDIX A: DERIVATION OF MAPPING BETWEEN CENTRAL SPIN MODEL AND LMG MODEL

In this Appendix, we give the derivation of the mapping between the central spin model and the LMG model. First of all, Eq. (2) can be rewritten as

$$H = H_0 + AV, \quad (A1)$$

where

$$H_0 = \frac{\Omega}{2}\sigma_z + \omega I_z, \quad (A2)$$

$$V = (1 + \lambda)I_x\sigma_x + (1 - \lambda)I_y\sigma_y. \quad (A3)$$

Note that  $H_0$  is diagonal with respect to the spin subspace while  $V$  is off-diagonal. Then we perform the Schrieffer-Wolff

transformation  $e^S$  on Eq. (A1) and obtain [84,85]

$$H' = e^{-S} H e^S = \sum_{k=0}^{\infty} \frac{1}{k!} [H, S]^{(k)}, \quad (\text{A4})$$

where  $[H, S]^{(k)} = [[H, S]^{(k-1)}, S]$ ,  $[H, S]^{(0)} = H$ , and the generator  $S$  is an anti-Hermitian and block-off-diagonal operator. In order to diagonalize the Hamiltonian  $H'$ , we need the block-off-diagonal part of  $H'$  to be zero up to second order in  $A$ , which leads to the follow relationship

$$[H_0, S] = -AV, \quad (\text{A5})$$

and we find the expression of  $S$  satisfying Eq. (A5) is as follows,

$$S = -i \frac{A(1+\lambda)}{\Omega} I_x \sigma_y + i \frac{A(1-\lambda)}{\Omega} I_y \sigma_x. \quad (\text{A6})$$

In the limit of  $\eta \rightarrow \infty$ , the Hamiltonian in Eq. (A4) becomes

$$\begin{aligned} H' &= H_0 + \frac{A}{2} [V, S] \\ &= \frac{\Omega}{2} \sigma_z + \left[ \omega - A^2 \frac{(1+\lambda)(1-\lambda)}{\Omega} \right] I_z \\ &\quad + A^2 \left[ \frac{(1+\lambda)^2}{\Omega} I_x^2 \sigma_z + \frac{(1-\lambda)^2}{\Omega} I_y^2 \sigma_z \right]. \end{aligned} \quad (\text{A7})$$

Furthermore, we set  $\tilde{g} = 2A\sqrt{N/\Omega\omega}$ ,  $\gamma_x = \tilde{g}^2 \omega (1+\lambda)^2/4$ ,  $\gamma_y = \tilde{g}^2 \omega (1-\lambda)^2/4$ , and finally we get the Hamiltonian in Eq. (4), which precisely corresponds to the Hamiltonian of the anisotropic LMG model.

## APPENDIX B: DERIVATION OF SPIN-SQUEEZING PARAMETER IN DYNAMICAL PROCESS

First of all, we give the derivation of Eqs. (17) and (18). For the ground state of the isotropic central spin model, the mean spin direction is always along the  $z$  axis, thus we have  $\langle I_x \rangle = \langle I_y \rangle = 0$ , and then we obtain [25]

$$\begin{aligned} \min(\Delta^2 I_{\bar{n}_\perp}) &= \frac{1}{2} [(I_x^2 + I_y^2) - \sqrt{((I_x^2 - I_y^2))^2 + 4 \text{Cov}(I_x, I_y)^2}] \\ &= \frac{1}{2} \langle I_x^2 + I_y^2 \rangle, \end{aligned} \quad (\text{B1})$$

where  $\text{Cov}(I_x, I_y) = \frac{1}{2} \langle I_x I_y + I_y I_x \rangle$ .

For  $\eta \rightarrow \infty$ , we make an approximation that  $\tilde{P}_{\uparrow, n-1} \simeq 0$ ,  $\tilde{P}_{\downarrow, n} \simeq 1$ , and Eq. (B1) becomes

$$\begin{aligned} \min(\Delta^2 I_{\bar{n}_\perp}) &= \frac{1}{2} \langle I^2 - I_z^2 \rangle \\ &= -\frac{1}{2} \left( n - \frac{N}{2} \right)^2 + \frac{N^2}{8} + \frac{N}{4}. \end{aligned} \quad (\text{B2})$$

Utilizing Eq. (B2) we can get Eqs. (17) and (18).

Then we give the derivation of the time evolution of spin-squeezing parameters  $\xi_S^2$  and  $\xi_R^2$ . The initial state we choose is given in Eq. (19), and under the condition of  $\eta \gg 1$  we have

$$\langle I_z \rangle = \frac{N}{2} \cos \theta_0, \quad (\text{B3})$$

$$\langle I_z^2 \rangle = \frac{1}{8} N [N + 1 + (N - 1) \cos 2\theta_0]. \quad (\text{B4})$$

Then we make the following approximations:  $\Omega_n \simeq \Omega$ ,  $P_\downarrow^n \simeq e^{i\frac{\Omega n t}{2}}$ ,  $P_\uparrow^n \simeq 0$ , and  $\Omega_n \simeq \Omega + 2k_n A^2$ . We obtain

$$\begin{aligned} \langle I_+ \rangle &\simeq \sum_{n=0}^{N-1} C_{N-1}^n N \left( \cos^2 \frac{\theta_0}{2} \right)^n \left( \sin^2 \frac{\theta_0}{2} \right)^{N-1-n} e^{-i\frac{(N-2n)A^2 t}{\Omega}} e^{i\omega t} \cot \frac{\theta_0}{2} \\ &= \frac{1}{2} N e^{i(\omega - \frac{A^2}{\Omega})t} \left( \cos \frac{A^2 t}{\Omega} + i \sin \frac{A^2 t}{\Omega} \cos \theta_0 \right)^{N-1} \sin \theta_0, \end{aligned} \quad (\text{B5})$$

$$\begin{aligned} \langle I_+^2 \rangle &\simeq e^{2i\omega t} \sum_{n=0}^{N-1} \left( \cos^2 \frac{\theta_0}{2} \right)^n \left( \sin^2 \frac{\theta_0}{2} \right)^{N-n} C_{N-2}^n N(N-1) e^{-\frac{i2(N-2n-1)A^2 t}{\Omega}} \cot^2 \frac{\theta_0}{2} \\ &= \frac{1}{4} e^{2i(\omega - \frac{A^2}{\Omega})t} N(N-1) \left[ \cos \left( \frac{2A^2 t}{\Omega} \right) + i \cos \theta_0 \sin \left( \frac{2A^2 t}{\Omega} \right) \right]^{N-2} \sin^2 \theta_0, \end{aligned} \quad (\text{B6})$$

$$\begin{aligned} 2\langle I_+ I_z \rangle + \langle I_+ \rangle &\simeq \sum_{n=0}^{N-1} C_{N-1}^n N \left( \cos^2 \frac{\theta_0}{2} \right)^n \left( \sin^2 \frac{\theta_0}{2} \right)^{N-n} e^{-i\frac{(N-2n)A^2 t}{\Omega}} e^{i\omega t} \left[ 2 \left( -\frac{N}{2} + n \right) + 1 \right] \cot \frac{\theta_0}{2} \\ &= \frac{1}{2} e^{i(\omega - \frac{A^2}{\Omega})t} N(N-1) \left[ \cos \left( \frac{A^2 t}{\Omega} \right) + i \cos \theta_0 \sin \left( \frac{A^2 t}{\Omega} \right) \right]^{N-2} \left[ \cos \theta_0 \cos \left( \frac{A^2 t}{\Omega} \right) + i \sin \left( \frac{A^2 t}{\Omega} \right) \right] \sin \theta_0. \end{aligned} \quad (\text{B7})$$

For the sake of simplicity, we choose  $\theta_0 = \pi/2$ , and the directions perpendicular to the mean spin direction  $\bar{n}_0$  are  $\bar{n}_1 = (-\sin \phi, \cos \phi, 0)$ ,  $\bar{n}_2 = (0, 0, 1)$ , and  $\phi = \omega t$ . Therefore, the spin-squeezing parameter is given by [25]

$$\begin{aligned} \xi_S^2 &= \frac{2}{N} [(I_{\bar{n}_1}^2 + I_{\bar{n}_2}^2) - \sqrt{((I_{\bar{n}_1}^2 - I_{\bar{n}_2}^2))^2 + 4 \text{Cov}(I_{\bar{n}_1}, I_{\bar{n}_2})^2}] \\ &= \frac{2}{N} (C - \sqrt{A^2 + B^2}), \end{aligned} \quad (\text{B8})$$

where

$$\mathcal{A} = \frac{1}{8}(N-1)N \left[ 1 - \cos \left( \frac{A^2 t}{\Omega} \right)^{N-2} \right], \quad (\text{B9})$$

$$\mathcal{B} = \frac{N}{2}(N-1) \cos \left( \frac{A^2 t}{\Omega} \right)^{N-2} \sin \left( \frac{A^2 t}{\Omega} \right), \quad (\text{B10})$$

$$\mathcal{C} = \mathcal{A} + \frac{N}{2}. \quad (\text{B11})$$

By substituting Eqs. (B9)–(B11) into Eq. (20), we can obtain the analytical solution for the time evolution of the spin-squeezing parameter  $\xi_S^2$ .

- 
- [1] M. A. Taylor and W. P. Bowen, Quantum metrology and its application in biology, *Phys. Rep.* **615**, 1 (2016).
- [2] M. A. Taylor, J. Janousek, V. Daria, J. Knittel, B. Hage, H.-A. Bachor, and W. P. Bowen, Biological measurement beyond the quantum limit, *Nat. Photonics* **7**, 229 (2013).
- [3] M. B. Nasr, D. P. Goode, N. Nguyen, G. Rong, L. Yang, B. M. Reinhard, B. E. Saleh, and M. C. Teich, Quantum optical coherence tomography of a biological sample, *Opt. Commun.* **282**, 1154 (2009).
- [4] P. A. Morris, R. S. Aspden, J. E. C. Bell, R. W. Boyd, and M. J. Padgett, Imaging with a small number of photons, *Nat. Commun.* **6**, 5913 (2015).
- [5] S. Qvarfort, A. Serafini, P. F. Barker, and S. Bose, Gravimetry through non-linear optomechanics, *Nat. Commun.* **9**, 3690 (2018).
- [6] S. Templier, P. Cheiney, Q. d'Armagnac de Castanet, B. Gouraud, H. Porte, F. Napolitano, P. Bouyer, B. Battelier, and B. Barrett, Tracking the vector acceleration with a hybrid quantum accelerometer triad, *Sci. Adv.* **8**, eadd3854 (2022).
- [7] G. Lamporesi, A. Bertoldi, L. Cacciapuoti, M. Prevedelli, and G. M. Tino, Determination of the Newtonian gravitational constant using atom interferometry, *Phys. Rev. Lett.* **100**, 050801 (2008).
- [8] S. W. Chiow, S. Herrmann, S. Chu, and H. Müller, Noise-immune conjugate large-area atom interferometers, *Phys. Rev. Lett.* **103**, 050402 (2009).
- [9] J. M. McGuirk, G. T. Foster, J. B. Fixler, M. J. Snadden, and M. A. Kasevich, Sensitive absolute-gravity gradiometry using atom interferometry, *Phys. Rev. A* **65**, 033608 (2002).
- [10] A. Sørensen and K. Mølmer, Spin-spin interaction and spin squeezing in an optical lattice, *Phys. Rev. Lett.* **83**, 2274 (1999).
- [11] D. Döring, G. McDonald, J. E. Debs, C. Figl, P. A. Altin, H.-A. Bachor, N. P. Robins, and J. D. Close, Quantum-projection-noise-limited interferometry with coherent atoms in a Ramsey-type setup, *Phys. Rev. A* **81**, 043633 (2010).
- [12] A. André, A. S. Sørensen, and M. D. Lukin, Stability of atomic clocks based on entangled atoms, *Phys. Rev. Lett.* **92**, 230801 (2004).
- [13] G. S. Agarwal and M. O. Scully, Ramsey spectroscopy with nonclassical light sources, *Phys. Rev. A* **53**, 467 (1996).
- [14] S. Chu, Atom interferometry, in *Coherent Atomic Matter Waves*, edited by R. Kaiser, C. Westbrook, and F. David (Springer, Berlin, 2001), pp. 317–370.
- [15] G. Xu and D. J. Heinzen, State-selective Rabi and Ramsey magnetic resonance line shapes, *Phys. Rev. A* **59**, R922 (1999).
- [16] V. Meyer, M. A. Rowe, D. Kielpinski, C. A. Sackett, W. M. Itano, C. Monroe, and D. J. Wineland, Experimental demonstration of entanglement-enhanced rotation angle estimation using trapped ions, *Phys. Rev. Lett.* **86**, 5870 (2001).
- [17] G. A. Smith, S. Chaudhury, A. Silberfarb, I. H. Deutsch, and P. S. Jessen, Continuous weak measurement and nonlinear dynamics in a cold spin ensemble, *Phys. Rev. Lett.* **93**, 163602 (2004).
- [18] D. Walls and P. Zoller, Enhanced sensitivity of a gravitational wave detector, *Phys. Lett. A* **85**, 118 (1981).
- [19] J. A. Dunningham and K. Burnett, Sub-shot-noise-limited measurements with Bose-Einstein condensates, *Phys. Rev. A* **70**, 033601 (2004).
- [20] K. Goda, O. Miyakawa, E. E. Mikhailov, S. Saraf, R. Adhikari, K. McKenzie, R. Ward, S. Vass, A. J. Weinstein, and N. Mavalvala, A quantum-enhanced prototype gravitational-wave detector, *Nat. Phys.* **4**, 472 (2008).
- [21] X. Wang and B. C. Sanders, Spin squeezing and pairwise entanglement for symmetric multiqubit states, *Phys. Rev. A* **68**, 012101 (2003).
- [22] A. S. Sørensen and K. Mølmer, Entanglement and extreme spin squeezing, *Phys. Rev. Lett.* **86**, 4431 (2001).
- [23] G. Tóth, C. Knapp, O. Gühne, and H. J. Briegel, Spin squeezing and entanglement, *Phys. Rev. A* **79**, 042334 (2009).
- [24] J. Estève, C. Gross, A. Weller, S. Giovanazzi, and M. K. Oberthaler, Squeezing and entanglement in a Bose-Einstein condensate, *Nature (London)* **455**, 1216 (2008).
- [25] J. Ma, X. Wang, C. Sun, and F. Nori, Quantum spin squeezing, *Phys. Rep.* **509**, 89 (2011).
- [26] A. Sørensen, L.-M. Duan, J. I. Cirac, and P. Zoller, Many-particle entanglement with Bose-Einstein condensates, *Nature (London)* **409**, 63 (2001).
- [27] C. Orzel, A. K. Tuchman, M. L. Fenselau, M. Yasuda, and M. A. Kasevich, Squeezed states in a Bose-Einstein condensate, *Science* **291**, 2386 (2001).
- [28] C. K. Law, H. T. Ng, and P. T. Leung, Coherent control of spin squeezing, *Phys. Rev. A* **63**, 055601 (2001).
- [29] U. V. Poulsen and K. Mølmer, Positive- $P$  simulations of spin squeezing in a two-component Bose condensate, *Phys. Rev. A* **64**, 013616 (2001).



- [30] D. Jaksch, J. I. Cirac, and P. Zoller, Dynamically turning off interactions in a two-component condensate, *Phys. Rev. A* **65**, 033625 (2002).
- [31] A. Micheli, D. Jaksch, J. I. Cirac, and P. Zoller, Many-particle entanglement in two-component Bose-Einstein condensates, *Phys. Rev. A* **67**, 013607 (2003).
- [32] M. Jääskeläinen, W. Zhang, and P. Meystre, Limits to phase resolution in matter-wave interferometry, *Phys. Rev. A* **70**, 063612 (2004).
- [33] S. Choi and N. P. Bigelow, Quantum squeezing and entanglement in a two-mode Bose-Einstein condensate with time-dependent Josephson-like coupling, *Phys. Rev. A* **72**, 033612 (2005).
- [34] M. Jääskeläinen and P. Meystre, Dynamics of Bose-Einstein condensates in double-well potentials, *Phys. Rev. A* **71**, 043603 (2005).
- [35] G.-R. Jin and S. W. Kim, Storage of spin squeezing in a two-component Bose-Einstein condensate, *Phys. Rev. Lett.* **99**, 170405 (2007).
- [36] G.-R. Jin and S. W. Kim, Spin squeezing and maximal-squeezing time, *Phys. Rev. A* **76**, 043621 (2007).
- [37] D. J. Wineland, J. J. Bollinger, W. M. Itano, F. L. Moore, and D. J. Heinzen, Spin squeezing and reduced quantum noise in spectroscopy, *Phys. Rev. A* **46**, R6797 (1992).
- [38] J. Hald, J. L. Sørensen, C. Schori, and E. S. Polzik, Spin squeezed atoms: A macroscopic entangled ensemble created by light, *Phys. Rev. Lett.* **83**, 1319 (1999).
- [39] B. Julsgaard, A. Kozhekin, and E. S. Polzik, Experimental long-lived entanglement of two macroscopic objects, *Nature (London)* **413**, 400 (2001).
- [40] K. Hammerer, A. S. Sørensen, and E. S. Polzik, Quantum interface between light and atomic ensembles, *Rev. Mod. Phys.* **82**, 1041 (2010).
- [41] G. M. Palma and P. L. Knight, Phase-sensitive population decay: The two-atom Dicke model in a broadband squeezed vacuum, *Phys. Rev. A* **39**, 1962 (1989).
- [42] A. Banerjee, Generation of atomic-squeezed states in an optical cavity with an injected squeezed vacuum, *Phys. Rev. A* **54**, 5327 (1996).
- [43] A. Kuzmich, L. Mandel, J. Janis, Y. E. Young, R. Eijnisman, and N. P. Bigelow, Quantum nondemolition measurements of collective atomic spin, *Phys. Rev. A* **60**, 2346 (1999).
- [44] J. L. Sørensen, J. Hald, and E. S. Polzik, Quantum noise of an atomic spin polarization measurement, *Phys. Rev. Lett.* **80**, 3487 (1998).
- [45] L. Vernac, M. Pinard, and E. Giacobino, Spin squeezing in two-level systems, *Phys. Rev. A* **62**, 063812 (2000).
- [46] A. Dantan and M. Pinard, Quantum-state transfer between fields and atoms in electromagnetically induced transparency, *Phys. Rev. A* **69**, 043810 (2004).
- [47] M. H. Schleier-Smith, I. D. Leroux, and V. Vuletić, Squeezing the collective spin of a dilute atomic ensemble by cavity feedback, *Phys. Rev. A* **81**, 021804(R) (2010).
- [48] Z. Zhang, L. Shao, W. Lu, Y. Su, Y.-P. Wang, J. Liu, and X. Wang, Single-photon-triggered spin squeezing with decoherence reduction in optomechanics via phase matching, *Phys. Rev. A* **104**, 053517 (2021).
- [49] J. Geremia, J. K. Stockton, and H. Mabuchi, Real-time quantum feedback control of atomic spin-squeezing, *Science* **304**, 270 (2004).
- [50] M. H. Schleier-Smith, I. D. Leroux, and V. Vuletić, States of an ensemble of two-level atoms with reduced quantum uncertainty, *Phys. Rev. Lett.* **104**, 073604 (2010).
- [51] A. E. Kozhekin, K. Mølmer, and E. Polzik, Quantum memory for light, *Phys. Rev. A* **62**, 033809 (2000).
- [52] A. Kuzmich, L. Mandel, and N. P. Bigelow, Generation of spin squeezing via continuous quantum nondemolition measurement, *Phys. Rev. Lett.* **85**, 1594 (2000).
- [53] I. D. Leroux, M. H. Schleier-Smith, and V. Vuletić, Implementation of cavity squeezing of a collective atomic spin, *Phys. Rev. Lett.* **104**, 073602 (2010).
- [54] T. Hernández Yanes, M. Płodzień, M. Mackoito Sinkevičienė, G. Žlabys, G. Juzeliūnas, and E. Witkowska, One- and two-axis squeezing via laser coupling in an atomic Fermi-Hubbard model, *Phys. Rev. Lett.* **129**, 090403 (2022).
- [55] L. Pezzè, A. Smerzi, M. K. Oberthaler, R. Schmied, and P. Treutlein, Quantum metrology with nonclassical states of atomic ensembles, *Rev. Mod. Phys.* **90**, 035005 (2018).
- [56] S. Kolkowitz, S. L. Bromley, T. Bothwell, M. L. Wall, G. E. Marti, A. P. Koller, X. Zhang, A. M. Rey, and J. Ye, Spin-orbit-coupled fermions in an optical lattice clock, *Nature (London)* **542**, 66 (2017).
- [57] M. S. Rudner, L. M. K. Vandersypen, V. Vuletić, and L. S. Levitov, Generating entanglement and squeezed states of nuclear spins in quantum dots, *Phys. Rev. Lett.* **107**, 206806 (2011).
- [58] H. Lipkin, N. Meshkov, and A. Glick, Validity of many-body approximation methods for a solvable model: (I). Exact solutions and perturbation theory, *Nucl. Phys.* **62**, 188 (1965).
- [59] S. Dooley, F. McCrossan, D. Harland, M. J. Everitt, and T. P. Spiller, Collapse and revival and cat states with an  $N$ -spin system, *Phys. Rev. A* **87**, 052323 (2013).
- [60] W.-B. He, S. Chesi, H.-Q. Lin, and X.-W. Guan, Exact quantum dynamics of XXZ central spin problems, *Phys. Rev. B* **99**, 174308 (2019).
- [61] L. Shao, R. Zhang, W. Lu, Z. Zhang, and X. Wang, Quantum phase transition in the XXZ central spin model, *Phys. Rev. A* **107**, 013714 (2023).
- [62] A. V. Khaetskii, D. Loss, and L. Glazman, Electron spin decoherence in quantum dots due to interaction with nuclei, *Phys. Rev. Lett.* **88**, 186802 (2002).
- [63] M. Bortz, S. Eggert, C. Schneider, R. Stübner, and J. Stolze, Dynamics and decoherence in the central spin model using exact methods, *Phys. Rev. B* **82**, 161308(R) (2010).
- [64] M. Bortz and J. Stolze, Exact dynamics in the inhomogeneous central-spin model, *Phys. Rev. B* **76**, 014304 (2007).
- [65] G.-Q. Liu, J. Xing, W.-L. Ma, P. Wang, C.-H. Li, H. C. Po, Y.-R. Zhang, H. Fan, R.-B. Liu, and X.-Y. Pan, Single-shot readout of a nuclear spin weakly coupled to a nitrogen-vacancy center at room temperature, *Phys. Rev. Lett.* **118**, 150504 (2017).
- [66] E. M. Kessler, G. Giedke, A. Imamoglu, S. F. Yelin, M. D. Lukin, and J. I. Cirac, Dissipative phase transition in a central spin system, *Phys. Rev. A* **86**, 012116 (2012).
- [67] S. Dusuel and J. Vidal, Continuous unitary transformations and finite-size scaling exponents in the Lipkin-Meshkov-Glick model, *Phys. Rev. B* **71**, 224420 (2005).

- [68] J. Ma and X. Wang, Fisher information and spin squeezing in the Lipkin-Meshkov-Glick model, *Phys. Rev. A* **80**, 012318 (2009).
- [69] M. Kitagawa and M. Ueda, Squeezed spin states, *Phys. Rev. A* **47**, 5138 (1993).
- [70] D. J. Wineland, J. J. Bollinger, W. M. Itano, and D. J. Heinzen, Squeezed atomic states and projection noise in spectroscopy, *Phys. Rev. A* **50**, 67 (1994).
- [71] G. Vitagliano, I. Apellaniz, I. L. Egusquiza, and G. Tóth, Spin squeezing and entanglement for an arbitrary spin, *Phys. Rev. A* **89**, 032307 (2014).
- [72] J. K. Korbicz, J. I. Cirac, and M. Lewenstein, Spin squeezing inequalities and entanglement of  $N$  qubit states, *Phys. Rev. Lett.* **95**, 120502 (2005).
- [73] G. Tóth, C. Knapp, O. Gühne, and H. J. Briegel, Optimal spin squeezing inequalities detect bound entanglement in spin models, *Phys. Rev. Lett.* **99**, 250405 (2007).
- [74] G. Vitagliano, P. Hyllus, I. L. Egusquiza, and G. Tóth, Spin squeezing inequalities for arbitrary spin, *Phys. Rev. Lett.* **107**, 240502 (2011).
- [75] M. Block, B. Ye, B. Roberts, S. Chern, W. Wu, Z. Wang, L. Pollet, E. J. Davis, B. I. Halperin, and N. Y. Yao, A universal theory of spin squeezing, [arXiv:2301.09636](https://arxiv.org/abs/2301.09636).
- [76] G.-R. Jin, Y.-C. Liu, and W.-M. Liu, Spin squeezing in a generalized one-axis twisting model, *New J. Phys.* **11**, 073049 (2009).
- [77] L. Pezzé and A. Smerzi, Entanglement, nonlinear dynamics, and the Heisenberg limit, *Phys. Rev. Lett.* **102**, 100401 (2009).
- [78] L.-G. Huang, F. Chen, X. Li, Y. Li, R. Lü, and Y.-C. Liu, Dynamic synthesis of Heisenberg-limited spin squeezing, *npj Quantum Inf.* **7**, 168 (2021).
- [79] L.-G. Huang, X. Zhang, Y. Wang, Z. Hua, Y. Tang, and Y.-C. Liu, Heisenberg-limited spin squeezing in coupled spin systems, *Phys. Rev. A* **107**, 042613 (2023).
- [80] J. Vidal, G. Palacios, and R. Mosseri, Entanglement in a second-order quantum phase transition, *Phys. Rev. A* **69**, 022107 (2004).
- [81] S.-J. GU, Fidelity approach to quantum phase transitions, *Int. J. Mod. Phys. B* **24**, 4371 (2010).
- [82] X.-Y. Chen, Y.-F. Xie, and Q.-H. Chen, Quantum criticality of the Rabi-Stark model at finite frequency ratios, *Phys. Rev. A* **102**, 063721 (2020).
- [83] H.-M. Kwok, W.-Q. Ning, S.-J. Gu, and H.-Q. Lin, Quantum criticality of the Lipkin-Meshkov-Glick model in terms of fidelity susceptibility, *Phys. Rev. E* **78**, 032103 (2008).
- [84] M.-J. Hwang, R. Puebla, and M. B. Plenio, Quantum phase transition and universal dynamics in the Rabi model, *Phys. Rev. Lett.* **115**, 180404 (2015).
- [85] M.-J. Hwang and M. B. Plenio, Quantum phase transition in the finite Jaynes-Cummings, *Phys. Rev. Lett.* **117**, 123602 (2016).